Controlling thermo-optic response in microresonators using bimaterial cantilevers

Biswajeet Guha[1] and Michal Lipson[1,2,*]

[1]*Electrical & Computer Engineering Department, Cornell University, Ithaca, New York 14853, USA*

[2]*Kavli Institute at Cornell for Nanoscience, Ithaca, New York 14853, USA*

**Corresponding author: ml292@cornell.edu*

Received September 22, 2014; revised November 20, 2014; accepted November 21, 2014; posted November 24, 2014 (Doc. ID 223587); published December 24, 2014

We demonstrate a novel platform to control the thermo-optic sensitivity in nanophotonic devices by evanescent coupling of light with bimaterial cantilevers. The cantilever can be designed to provide a negative thermal feedback to passively compensate for the positive thermo-optic effect in the waveguide core. We demonstrate athermal operation over 14 deg in cantilever coupled Silicon ring resonators, limited only by fabrication tolerances. We also show how the same platform can provide positive thermal feedback and overcome the material thermo-optic limit for increasing sensitivity of resonant detectors and thermal imagers. © 2014 Optical Society of America

OCIS codes: (230.5750) Resonators; (120.4880) Optomechanics; (120.6780) Temperature; (040.6808) Thermal (uncooled) IR detectors, arrays and imaging.

http://dx.doi.org/10.1364/OL.40.000103

Thermal sensitivity of optical microresonators is one the major bottlenecks for technology implementation of silicon photonics. The sensitivity of any photonic structure to ambient temperature fluctuations is caused by the change in material refractive index with temperature, which is called thermo-optic (TO) effect [1]. A thermo-optic coefficient of Si (1.86×10^{-4} K^{-1}) is almost an order of magnitude higher than that of most other commonly used photonic materials (SiO_2, Si_3N_4, etc.). This leads to a resonance sensitivity of ~0.1 nm/K for an optical mode tightly confined in Si, irrespective of device design or dimension. This sensitivity is frequently exploited to tune the resonance wavelength [2] or make sensitive detectors and thermal imagers [3]. However, this temperature sensitivity also makes Si photonic devices extremely unstable in integrated platforms [4]. For example, the resonance wavelength of an Si ring resonator, with a moderate quality factor of 10,000, will shift by one linewidth with only 1°C change in temperature.

Most of the approaches proposed to overcome the problem of temperature sensitivity in Si photonics are power hungry, CMOS-incompatible, or lead to delocalized optical modes. Temperature stabilization schemes using negative thermo-optic coefficient based polymers are not compatible with front-end CMOS processing and lead to delocalized optical modes [5–7]. Active stabilization involving sensors and heaters can be extremely power hungry, especially since heaters need to be placed far from the optical mode to avoid metal induced losses [8–12]. Recently, there have been novel demonstrations of thermal stabilization of a resonator by coupling it to a larger interferometer which counteracts the thermally induced phase change in the resonator [13–16]. This scheme is CMOS-compatible and passive, but needs an extra footprint for the interferometer. Finally, recent works have used TiO_2 as cladding, which has an inherent negative TO effect to counter the positive TO effect of Si [17–20]. The drawback of this scheme is that the optical mode needs to be delocalized and any further tuning or modulation becomes extremely power hungry.

While some schemes have been proposed and implemented to reduce the TO effect in photonic devices, very limited work has been done to fully control the TO effect or even increase the temperature sensitivity for certain applications. The primary reason is that the upper limit in thermal sensitivity of photonic devices is a fundamental material constant (TO coefficient), which is set by sensitivity of the material bandgap to temperature because of electron–phonon coupling, lattice expansion coefficients [21], etc. In practice, measured thermal sensitivities are slightly lower than this upper limit because only part of the optical mode is confined in the waveguide core. Hence, applications that need high thermal sensitivities, like thermal tuning and thermal detectors [3,22,23], are also constrained in their sensitivity/efficiency by this upper limit.

In this Letter, we present a platform that achieves full control over the thermo-optic response of a resonator, independent of the material TO coefficients, based on evanescent coupling between a bimaterial cantilever and an optical resonator. Cantilevers have previously been coupled to microresonators for achieving ultralow power wavelength tuning [24] or for decoupling optical and mechanical resonators in optomechanics [25–28], but not in the context of manipulating thermal properties. Bimaterial cantilevers have been used for ultra-sensitive temperature measurements, such as near-field radiative heat transfer [29,30]. In the proposed platform, the bimaterial cantilever deflects with change in temperature because of thermal stress, which provides a feedback to the resonator. The gap between the cantilever and the resonator can be adjusted to control the strength of this feedback. Figure 1(a) shows a schematic of a ring resonator with a bimaterial cantilever on top. For simplicity we chose a circular cantilever, though other designs can be similarly implemented. Figure 1(b) shows a cross section of the waveguide, which has an Si core; the cantilever is made of Si on the top and Al_2O_3 at the bottom. This particular cantilever is designed to provide a negative thermal feedback and lower the overall temperature sensitivity of the resonator. Note that one could

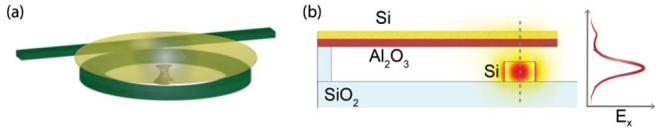

Fig. 1. (a) Schematic of the proposed platform: a bimaterial cantilever is evanescently coupled to the resonator waveguide. (b) Cross-section view and TE polarized optical mode of the coupled cantilever-waveguide system. The e-field along the dashed line is also shown.

use the same principle for increasing the temperature sensitivity by reversing the order of material layers in the cantilever. The e-field distribution of the optical mode [Fig. 1(b) inset] shows that most of the field is still in the waveguide core, with only a small fraction delocalized in the cantilever.

Based on this concept, we show an athermal resonator where the thermo-mechanical response of the cantilever and the optomechanical coupling are designed to exactly cancel out the thermo-optic drift of the ring. The bimaterial cantilever is designed to bend upward as temperature increases, thereby decreasing the effective index of the coupled mode and counteracting the thermo-optic effect. This is achieved by ensuring that the bottom layer of the cantilever has a higher thermal expansion coefficient (α) than the top layer. In our specific design we chose Al_2O_3 ($\alpha = 8 \times 10^{-6}$ K^{-1}) and Silicon ($\alpha = 3 \times 10^{-6}$ K^{-1}), each 100 nm thick. Figure 2(a) shows the strength of the optomechanical coupling. When the cantilever is far from the waveguide, the optical mode is minimally perturbed by change in cantilever position. An effective index (n_{eff}) of the coupled mode increases strongly as the gap is reduced. The strength of this coupling can be engineered by refractive indices of the layers, material thicknesses, and the initial gap. Figure 2(b) shows the change in effective mode index of the TE mode ($n_{\text{eff}} \sim 2.27$) as a function of temperature for several different gaps. It is evident that when the gap is large enough (>400 nm) n_{eff} increases with temperature at a rate of $\sim 2 \times 10^{-4}$ K^{-1}, dominated by the TO effect in the waveguide core. At very small gaps (<250 nm), n_{eff} strongly decreases with temperature. At some intermediate gaps (250–350 nm), where coupling is just right for thermal deflection of cantilever to cancel out refractive index changes in the waveguide, the change in n_{eff} is minimal with change in temperature.

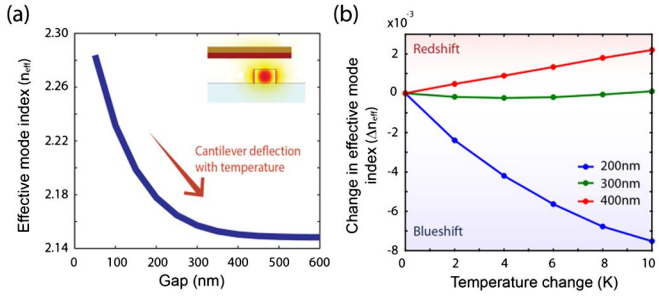

Fig. 2. (a) Effective index of the coupled optical mode as a function of coupling gap. (b) Change in effective index of the optical mode as a function of temperature for different coupling gaps of the cantilever. When the cantilever is far from the resonator waveguide, the change in the effective index is positive and close to the TO limit ($\sim 2 \times 10^{-4}$ K^{-1}). As the coupling gap is reduced, the cantilever interacts strongly with the optical mode and causes giant negative change. One can see that there is an optimum coupling gap where change in n_{eff} with temperature is minimal.

Si ring resonators with properly designed circular bimaterial cantilevers were fabricated on a silicon-on-insulator (SOI) wafer with 240 nm Si device layer and 3 μm buried oxide layer (BOX). Waveguides were defined using electron beam lithography and etched in a $C_4F_8/SF_6/Ar/O_2$ chemistry. A 10 nm Si slab was left behind to isolate the buried oxide layer from the subsequent release step. The device was cladded with 50 nm Al_2O_3 deposited using Atomic Layer Deposition. This Al_2O_3 layer encapsulates the Si and further protects the BOX layer from the release step. 300 nm SiO_2 was deposited using plasma enhanced chemical vapor deposition (PECVD) which defines the gap between the cantilever and the waveguide and will act as sacrificial layer during the cantilever release step. Circular cantilevers made of 100 nm thick Al_2O_3 and Si were deposited on top using electron beam evaporation and lift-off. Finally, the cantilevers were released in HF-vapor based dry isotropic etch to obtain free standing bimaterial cantilevers on top of unreleased Si ring resonators. Figure 3(a) shows a scanning electron microscope (SEM) image of the coupling region of the ring resonator with the cantilever on top. The deflection of the cantilever was measured using a temperature stage inside a SEM chamber. Figure 3(b) shows that the cantilever indeed deflects upward with increases in temperature because of a larger thermal expansion of the bottom layer. The deflection is exaggerated since the cantilever is heated to over 100 deg.

We demonstrate the ability to control the thermal sensitivity of the resonator, and capability of athermal operation over 14 deg, limited only by our fabrication

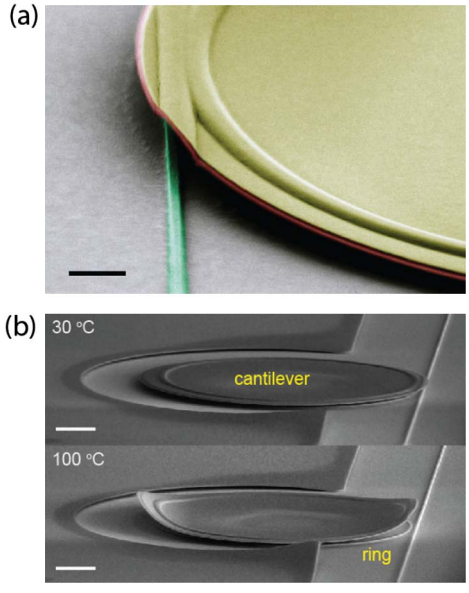

Fig. 3. (a) False-colored SEM image showing the coupling waveguide and the bimaterial cantilever. Scale bar is 2 μm. (b) Cantilever position at room temperature (above) and 100°C (below). Scale bar is 20 μm.

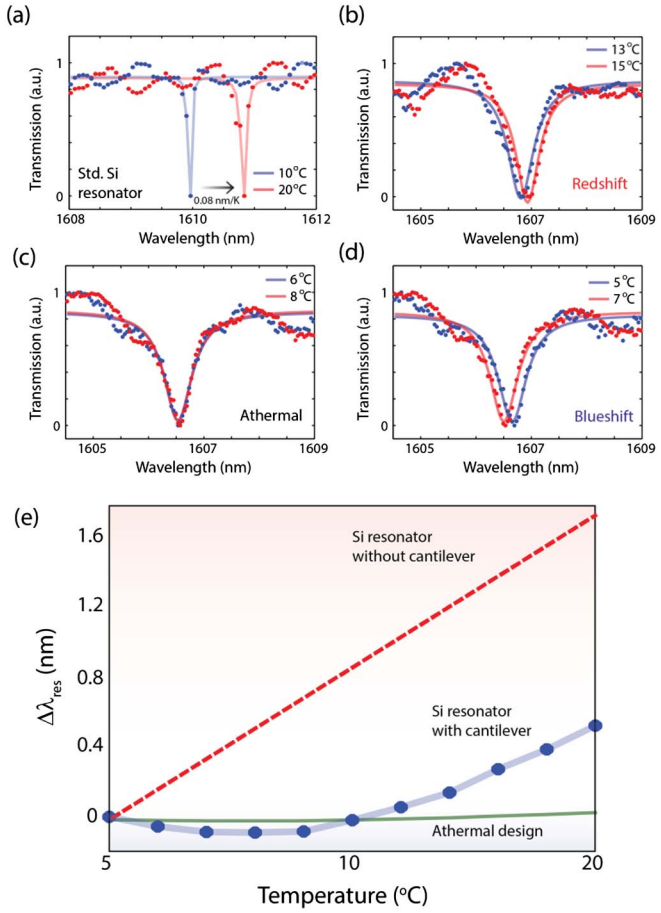

Fig. 4. (a) 0.08 nm/K redshift from a standard Si resonator. (b)–(d) Redshift, near-zero shift, and blueshift of resonances observed in a resonator coupled to a bimaterial cantilever. (e) Resonance sensitivity to temperature for Si resonator, with and without a compensating cantilever.

tolerance. A transmission spectrum of a 40 μm radius Si ring resonator was measured at different temperatures. For comparison, Fig. 4(a) shows the transmission spectrum of an Si resonator without any cantilever at two different temperatures. It shows a constant redshift of ~0.08 nm/K, set by the TO coefficient of Si. Figures 4(b)–4(d) show the spectra of a fabricated Si resonator coupled to a bimaterial cantilever on top, designed to provide a negative thermal feedback. At temperatures of 13°C and above [Fig. 4(b)], the gap between the cantilever and the waveguide is large enough such that the TO effect dominates and resonance redshifts with an increase in temperature. As temperature is reduced, the cantilever moves closer to the waveguide and the TO effect is compensated by refractive index change caused due to the mechanical deflection of the cantilever. This is the athermal operating regime [Fig. 4(c)]. Further reduction in temperature brings the cantilever even closer to the waveguide where the optomechanical shift dominates causing blueshift of resonance wavelength [Fig. 4(d)]. Figure 4(e) shows the resonance position over a wide temperature range. The resonance of a conventional resonator without any cantilever is shown in red. Temperature sensitivity in our cantilever coupled devices is significantly lower and changes sign as previously mentioned. The athermal operating range is around 14 deg (defined by the range where change in resonance wavelength is less than half of the linewidth). The green line in Fig. 4(e) shows athermal behavior for ideal coupling gap of 300 nm. In our devices, the cantilever bent up slightly during release because of residual stress, thus affecting the designed coupling gap. Accurate control of the coupling gap can extend athermal operation over a much wider temperature range.

The above platform could, in principle, be used to also enhance the thermo-optic response of photonic structures and break the material TO limit of Si based thermal/mid-IR all-optical detectors by over two orders of magnitude. The schematic of such a device is shown in Fig. 5(a), where an Si microresonator is evanescently coupled to a bimaterial cantilever made of Si and Al. Unlike the athermal design, this cantilever is designed to bend down with increase in temperature (Al has much higher thermal expansion coefficients ($\alpha_{Al} = 23 \times 10^{-6}$ K^{-1}) than Si ($\alpha_{Si} = 3 \times 10^{-6}$ K^{-1})). As temperature increases, the cantilever comes closer to the waveguide, increasing the effective index of the coupled optical mode, same as the TO effect. This positive feedback greatly enhances the overall temperature sensitivity. Figure 5(b) shows the temperature sensitivity of the resonance wavelength for different coupling gaps. For a modest coupling gap of 200 nm, the temperature sensitivity is ~1.9 nm/K, which is an enhancement of over two orders of magnitude compared to the thermo-optic limit of Si (~0.1 nm/K).

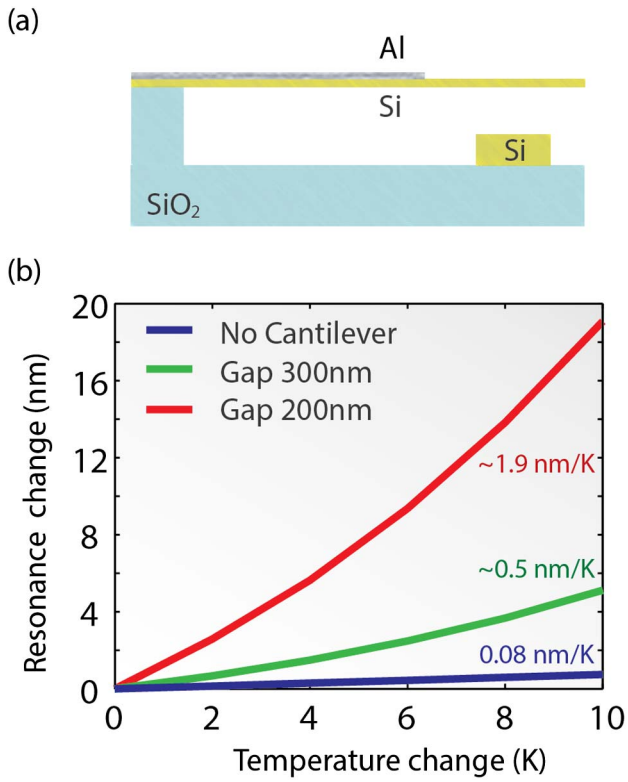

Fig. 5. (a) Cantilever design for enhanced thermo-optic response. (b) Temperature sensitivity of cavity resonance wavelength for different coupling gaps. At a gap of 200 nm, over two orders of magnitude enhancement in temperature sensitivity are expected.

In summary, we have presented a novel platform to accurately control the TO sensitivity of optical resonators. We demonstrated that this technique allows us to achieve athermal operation of any Si/SiN based microring resonator independent of cavity size or quality factor. The device is compact, CMOS-compatible (all materials including those used in the cantilever are compatible with the thermal budget of front-end CMOS), and has relatively large modal confinement in Si, in contrast to some of the previous works on attempting thermal stabilization using mode delocalization [5,18,19]. High confinement in Si is necessary for dense integration and low power tuning (thermo-optic or electro-optic). The mechanical design of the cantilever [31] (to linearize its deflection with temperature) and coupling gap can be optimized to yield a very large athermal operating range. The same platform can be modified to significantly enhance the TO sensitivity of photonic devices. This is especially important for thermal/mid-IR detectors, where the sensitivity is limited by optical quality factor, TO sensitivity, material absorption, and thermal isolation. The overall photonic structure can in principle have TO sensitivities two orders of magnitude higher than material TO limit.

References

1. Y. Varshni, Physica (Amsterdam) **34**, 149 (1967).
2. P. Dong, W. Qian, H. Liang, R. Shafiiha, D. Feng, G. Li, J. E. Cunningham, A. V. Krishnamoorthy, and M. Asghari, Opt. Express **18**, 20298 (2010).
3. M. R. Watts, M. J. Shaw, and G. N. Nielson, Nat. Photonics **1**, 632 (2007).
4. T. Zhang, J. L. Abellan, A. Joshi, and A. K. Coskun, *Design, Automation and Test in Europe Conference and Exhibition* (IEEE, 2014).
5. P. Alipour, E. S. Hosseini, A. A. Eftekhar, B. Momeni, and A. Adibi, *Conference on Lasers and Electro-Optics–Laser Applications to Photonic Applications* (Optical Society of America, 2009).
6. J. Teng, P. Dumon, W. Bogaerts, H. B. Zhang, X. G. Jian, X. Y. Han, M. S. Zhao, G. Morthier, and R. Baets, Opt. Express **17**, 14627 (2009).
7. M. Han and A. Wang, Opt. Lett. **32**, 1800 (2007).
8. C. T. DeRose, M. R. Watts, D. C. Trotter, D. L. Luck, G. N. Nielson, and R. W. Young, *Conference on Lasers and Electro-Optics–Laser Applications to Photonic Applications* (Optical Society of America, 2010).
9. S. Manipatruni, R. K. Dokania, B. Schmidt, N. Sherwood-Droz, C. B. Poitras, A. B. Apsel, and M. Lipson, Opt. Lett. **33**, 2185 (2008).
10. M. R. Watts, W. A. Zortman, D. C. Trotter, G. N. Nielson, D. L. Luck, and R. W. Young, *Conference on Lasers and Electro-Optics–Laser Applications to Photonic Applications* (Optical Society of America, 2009).
11. K. Padmaraju, D. F. Logan, X. Zhu, J. J. Ackert, A. P. Knights, and K. Bergman, Opt. Express **21**, 14342 (2013).
12. D. A. B. Miller, Proc. IEEE **97**, 1166 (2009).
13. B. Guha, A. Gondarenko, and M. Lipson, Opt. Express **18**, 1879 (2010).
14. B. Guha, B. B. C. Kyotoku, and M. Lipson, Opt. Express **18**, 3487 (2010).
15. B. Guha, K. Preston, and M. Lipson, Opt. Lett. **37**, 2253 (2012).
16. M. Uenuma and T. Motooka, Opt. Lett. **34**, 599 (2009).
17. J. Bovington, R. Wu, K.-T. Cheng, and J. E. Bowers, Opt. Express **22**, 661 (2014).
18. S. S. Djordjevic, K. Shang, B. Guan, S. T. Cheung, L. Liao, J. Basak, H.-F. Liu, and S. Yoo, Opt. Express **21**, 13958 (2013).
19. B. Guha, J. Cardenas, and M. Lipson, Opt. Express **21**, 26557 (2013).
20. F. Qiu, A. M. Spring, F. Yu, and S. Yokoyama, Appl. Phys. Lett. **102**, 051106 (2013).
21. K. O'Donnell and X. Chen, Appl. Phys. Lett. **58**, 2924 (1991).
22. C. Jha, G. Bahl, R. Melamud, S. Chandorkar, M. Hopcroft, B. Kim, M. Agarwal, J. Salvia, H. Mehta, and T. Kenny, Appl. Phys. Lett. **91**, 074101 (2007).
23. B.-B. Li, Q.-Y. Wang, Y.-F. Xiao, X.-F. Jiang, Y. Li, L. Xiao, and Q. Gong, Appl. Phys. Lett. **96**, 251109 (2010).
24. S. Abdulla, L. Kauppinen, M. Dijkstra, M. De Boer, E. Berenschot, H. Jansen, R. De Ridder, and G. Krijnen, Opt. Express **19**, 15864 (2011).
25. M. Li, W. H. Pernice, and H. X. Tang, Phys. Rev. Lett. **103**, 223901 (2009).
26. E. Gavartin, P. Verlot, and T. Kippenberg, Nat. Nanotechnol. **7**, 509 (2012).
27. S. Sridaran and S. A. Bhave, Opt. Express **19**, 9020 (2011).
28. K. Srinivasan, H. Miao, M. T. Rakher, M. Davanco, and V. Aksyuk, Nano Lett. **11**, 791 (2011).
29. E. Rousseau, A. Siria, G. Jourdan, S. Volz, F. Comin, J. Chevrier, and J. J. Greffet, Nat. Photonics **3**, 514 (2009).
30. S. Shen, A. Narayanaswamy, and G. Chen, Nano Lett. **9**, 2909 (2009).
31. S. H. Lim, J. Choi, R. Horowitz, and A. Majumdar, J. Microelectromech. Syst. **14**, 4 (2005).